# Structure and dynamics of *Candida rugosa* lipase: the role of organic solvent

Bimo Ario Tejo[1], Abu Bakar Salleh[1, 2], Juergen Pleiss[3 *]

[1]Department of Biochemistry and Microbiology,
[2]Institute of Bioscience, Universiti Putra Malaysia, 43400 Serdang, Selangor, Malaysia

[3]Institute of Technical Biochemistry, University of Stuttgart, Allmandring 31, 70569 Stuttgart, Germany

[*]To whom correspondence should be addressed
E-mail: Juergen.Pleiss@itb.uni-stuttgart.de
Tel: +49-711-685-3191, Fax: +49-711-685-3196

***Keywords:*** Lipase; lid movement; molecular dynamics simulation; organic solvent

***Abbreviations:*** CALB, *Candida antarctica* lipase B; CRL, *Candida rugosa* lipase; $CCl_4$, carbon tetrachloride; MD, molecular dynamics; PCL, *Pseudomonas cepacia* lipase; rmsd, root-mean square deviation(s).

**Abstract**

The effect of organic solvent to structure and dynamics of proteins was investigated by multiple molecular dynamics simulations (1 ns each) of *Candida rugosa* lipase in water and in carbon tetrachloride. The choice of solvent had only a minor structural effect. For both solvents the open and the closed conformation of the lipase were near to their experimental X-ray structures ($C_\alpha$ rms deviation 1-1.3 Å). However, the solvents had a highly specific effect on the flexibility of solvent-exposed side chains: polar side chains were more flexible in water, but less flexible in organic solvent. In contrast, hydrophobic residues were more flexible in organic solvent, but less flexible in water. As a major effect solvent changed the dynamics of the lid, a mobile element involved in activation of the lipase, which fluctuated as rigid body about its average position. While in water the deviations were about 1.6 Å, organic solvent reduced flexibility to 0.9 Å. This increase rigidity was caused by two salt bridges (Lys85-Asp284, Lys75-Asp79) and a stable hydrogen bond (Lys75-Asn 292) in organic solvent. Thus organic solvents stabilize the lid but render the side chains in the hydrophobic substrate binding site more mobile.

## Introduction

Nonaqueous enzymology has developed into an active and powerful area of research. [1] Exploitation of enzymes as highly selective biocatalysts in organic medium was fuelled by applications in asymmetric synthetic transformations of enantiopure pharmaceuticals. [2] Biochemical properties like activity, specificity, and selectivity have been shown to be dependent on the choice of organic solvent and water activity. [3] However, not much is known about the molecular mechanisms how organic solvents lead to a change of structure and dynamics of enzymes, and thus to changes of the experimentally observed biochemical properties.

One of the most interesting and well-investigated class of enzymes in this field are lipases (triacylglycerol hydrolases, EC 3.1.1.3). Lipases are activated upon contact with a nonpolar substrate phase which leads to opening of a mobile element, the lid. This "interfacial activation" is triggered by adsorption to the water-lipid interface, [4] even though it was proposed that interfacial activation does not necessarily happen in all lipases. [5] One of the enzymes which shows interfacial activation is *Candida rugosa* lipase (CRL). CRL is a versatile biocatalyst which catalyzes hydrolysis, alcoholysis, esterification and transesterification of triacylglycerols and other hydrophobic esters. [6] The crystal structure of this 57 kDa protein has been resolved at 2.06 and 2.1 Å resolutions with two different conformations, an open and a closed form. [7, 8] Like other microbial lipases, CRL is a member of the α/β-hydrolase fold family which consists of a central hydrophobic eight-stranded β-sheet packed between two layers of amphiphilic α-helices. A mobile lid region consists of two short α-helices linked to the body of the lipase by flexible elements. The lid consists of residues 62-92 and rotates by almost $90^{o}$ from the closed to the open conformation. In the closed, inactive conformation, it covers the substrate binding site. In the

open, active conformation, it extends away from the protein surface and makes the catalytic triad, Ser209, His449 and Glu341, accessible to substrate. Upon opening, the exposed substrate binding site and the inside of the lid form a large hydrophobic patch which is supposed to interact with the hydrophobic substrate interface.

Up to now there is no crystal structure of CRL in organic solvents, but for *Pseudomonas cepacia* lipase (PCL), *Candida antarctica* lipase B (CALB) and subtilisin Carlsberg, it has been shown that their crystal structures in organic solvent and water are essentially identical. [9, 10] However, major rearrangements occur in the side chain orientation, [10, 11] which in many cases is an important determinant of enzyme activity. [12] Another important effect of organic solvent is a change in protein flexibility. It has been shown experimentally that enzyme flexibility is correlated with enzyme activity and enantioselectivity in organic solvents. [13]

To investigate the effect of organic solvent on CRL on a molecular level, we performed molecular dynamics simulations of four models (the open and closed conformation of CRL solvated in two solvents each, water and carbon tetrachloride) and compared the effect of the two solvents on the average protein structure and flexibility of backbone and side chains.

## Materials and methods

### Hard- and software

Molecular dynamics (MD) simulations and energy minimizations were carried out on a 256 nodes PCs cluster (AMD Athlon 1.33 GHz, http://www.itb.uni-stuttgart.de/BioCortex/) based on a Beowulf architecture (Linux Mandrake 8.2) using the AMBER 7 suite of programs. [14] SwissPdb Viewer 3.7 and Sybyl (Tripos, St.Louis, MO) were used for structure visualization. Statistical analyses were done using Origin software (OriginLab, Northampton, MA).

### Structure preparation

The crystal structures of the open and closed conformations of *C. rugosa* lipase (entries 1CRL and 1TRH, respectively) were taken from the Protein Data Bank. [15] The structures are resolved to 2.06 Å (open) and 2.1 Å (closed). In these structures, three *N*-glucosamine residues which are covalently bound to the enzyme were removed prior to simulations. All water molecules were maintained. For simulation in organic solvent, a carbon tetrachloride ($CCl_4$) solvent box was built based on Fox and Kollman parameters [16] and saved as *.lib* file in Amber 7 library files.

### Molecular dynamics simulations

All systems were minimized using the steepest descent method followed by the conjugate gradient method. MD simulations were carried out with a time step of 1 fs with *parm99* force field implemented in Amber 7 program. SHAKE [17] was applied to all bonds involving hydrogen atoms with geometric tolerance of 0.00000001. Simulations were run with the Particle Mesh Ewald (PME) method. [18] For simulations in water, a truncated octahedral box of TIP3P water molecules (11,430 molecules) was built around the structure with a

minimal distance of 10 Å between the protein surface and the wall of the box. Simulations in organic solvents were performed in a truncated octahedral box of $CCl_4$ which consists of 1,667 molecules. Solvated systems were gradually heated to 300 K during 20 ps with constant volume and a temperature coupling constant of 0.2 ps. In the subsequent equilibration phase of 10 ps, the conditions were changed to constant pressure and the coupling constants were increased gradually. During the production phase of 970 ps, temperature and pressure coupling constants were 0.8 ps and 1.0 ps, respectively. Each system was simulated with five different initial velocities for total time of 1 ns.

Solvent accessible surface area (SASA) analysis

SASA analysis was performed using Gauss-Bonnet algorithm implemented in GETAREA 1.1 program (http://scsb.utmb.edu/getarea). Exposed and buried residues were described as a ratio value of side-chain surface area to solvent accessible area of the particular residue "X" in the tripeptide Gly-X-Gly in an ensemble of 30 random conformation. Percentage ratio more than 50% is classified as exposed residue.

Atomic fluctuation analysis

Atomic fluctuations can be estimated from the temperature factor (B-factor) through the relationship:

$$B_i = \frac{8\pi^2}{3}\left\langle \Delta r_i \right\rangle^2 \qquad (1)$$

where $\Delta r_i$ is the rms positional fluctuation of atom *i*. The simulated B-factors were calculated using the coordinates of the last 500 ps segment of the trajectories. To remove rotational and

translational movements during simulations, the trajectories were superposed to a reference structure at t=0.

Time-correlation analysis

Time-correlation functions provide a quantitative measure of the dynamic behaviour of the system. The time correlation functions of a vector from the center-of-mass of the protein core to the center-of-mass of the lid were calculated based on:

$$C(\tau) = \left\langle \frac{P_2\left(\cos\theta(t, t+\tau)\right)}{r^3(t)\, r^3(t+\tau)} \right\rangle_t \qquad (2)$$

where $P_2$ is the second-order Legendre polynomial, $\theta(t,t+\tau)$ is the angle between the vectors at two timepoints t and $t+\tau$, and r is length of the vector between the two centers of mass.

The time-correlation function of a diffusive motion of a vector can be represented by a linear combination of two exponential functions:

$$C(t) = C_0 + C_1 e^{-\frac{t}{\tau 1}} + C_2 e^{-\frac{t}{\tau 2}} \qquad (3)$$

where $\tau_1$ and $\tau_2$ correspond to the relaxation time of biphasic time-correlation function curves.

Analysis of scalar movements

Analysis of scalar movements of the lid core region was performed using the second-order Legendre polynomial through the equations:

$$P_2(t) = \frac{3}{2}\left\langle \cos^2 \theta_{ij}(t) \right\rangle - \frac{1}{2} \quad (4)$$

$$\Delta d = r_{ij} \sin \theta_{ij} \quad (5)$$

where $\theta_{ij}$ corresponds to the angle between vector *i* and *j*, Δd is the displacement of the lid, and $r_{ij}$ is the average distance between the centers-of-mass of protein core and the lid.

## Results

### Equilibration

Deviation of the simulated trajectory from the crystallographic structures in the open and closed conformation (Fig. 1) was monitored by calculating the root-mean square deviation (rmsd) as a function of time (Fig. 2a). All simulations reached equilibrium after 500 ps and remained stable for the next 500 ps. Each protein-solvent complex was simulated five times with different initial velocities. Averaged rmsd values for the last 500 ps of open CRL in water and $CCl_4$ were 1.0 $\pm$ 0.05 Å and 1.3 $\pm$ 0.05 Å, respectively, of closed CRL 0.95 $\pm$ 0.08 Å and 1.3 $\pm$ 0.17 Å, respectively.

Comparison of the open and closed conformation (PDB entries 1CRL and 1TRH, respectively) indicated that the core of the protein (508 $C_\alpha$ atoms of all 534 residues) superimposed with an RMS deviation of only 0.3 Å between the two crystal structures, while the positions of 26 $C_\alpha$ atoms of the lid differed significantly (Fig. 1). Restricting the rmsd analysis of the simulation to the core and excluding the lid resulted in similar rmsd values as for the whole structure: for the closed conformation 0.9 $\pm$ 0.07 Å and 1.2 $\pm$ 0.13 Å in water and $CCl_4$, respectively, while for the open conformation 1.0 $\pm$ 0.07 Å and 1.2 $\pm$ 0.04 Å in water and $CCl_4$, respectively.

To analyze how the system approaches the equilibrium, two-dimensional rmsd was analyzed. In contrast to one-dimensional rmsd which measures how far the solute moves away from its initial structure during the simulation, two-dimensional rmsd measures the deviation between any two conformations (Fig. 2b). Thus it monitors how the system moves from one local minimum to the other upon equilibration. As an example, in a simulation of closed CRL in $CCl_4$ the system seemed to reach equilibrium already after 200 ps as concluded from a one-dimensional rmsd analysis, while two-dimensional rmsd revealed

that the system moved along several local minima. A local minimum can be defined as a region of less than 0.7 Å rmsd of all conformers (green areas in Fig. 2b: 30-200 ps, 200-400 ps, 400-1000 ps), while the deviation between the local minima was more than 0.7 Å (yellow, red, white).

Flexibility

Analysis of simulated B-factors indicated that in all simulations residues of the lid region were more flexible than residues of the protein core (Fig. 3 and Fig. 4). However, open and closed CRL in water reached the highest B-factors at different residues: in the open CRL, Val81-Ser91 (located at the C-terminus of the lid) have highest mobility (Fig. 3a), while in the closed CRL residues Tyr69-Val81 (at the N-terminus of the lid) are most mobile (Fig. 4a). For open CRL, the values of simulated B-factors in water were generally lower than the experimentally determined crystallographic B-factors (Fig. 3a), except residues Ile18, Asn35, Lys52, Tyr69 to Leu73, Leu80, Lys85, Lys109, Lys231, Glu257, Ser270, Glu325, Tyr458, Lys488, Leu508 and Lys514. Most of these residues were hydrophilic amino acids. Similarly, values of simulated B-factors in $CCl_4$ were also generally lower than the experimentally determined crystallographic B-factors (Fig. 3b), except residues Val33, Leu36, Phe87, Met186, Ala271, Phe344, Leu396 to Leu399, Val444, Leu455, Leu486, Ala507 and Leu510 which were higher. In contrast to the water simulation, these residues were mainly hydrophobic amino acids.

Direct comparison of averaged B-factors for simulations of the open CRL in water and $CCl_4$ showed that most residues had similar B-factors except 41 mostly hydrophobic residues which had higher flexibility in $CCl_4$, while about 65 mostly polar residues had higher flexibility in water (Fig. 5a). Most of these residues were solvent exposed and located on the surface of the enzyme (Fig. 6a). However, 15 residues with higher flexibility in $CCl_4$ were

buried (Pro2, Gly124, Pro135, Ile139, Trp161, Met186, Asn314, Val333, Phe345, Met378, Leu410, Asp457, Ser462, Ile505 and Leu510), while five residues with higher flexibility in water were buried (Asp10, Leu179, Asp199, Glu208 and Tyr254). In most cases the side chain flexibility was affected. But for 24 residues, the flexibility of the backbone atoms changed: 10 residues had higher backbone flexibility in $CCl_4$ (Lys52, Val81, Ser84, Gly124, Pro135, Gly441, Leu442, Pro443, Val444 and Leu445), 14 residues in water (Ala1, Tyr69, Glu70, Glu71, Lys85, Val86, Glu88 Ala89, Pro106, Gly107, Gly269, Ser270, Gln387 and Ser440) (Fig. 6a). The residues which show increased flexibility in $CCl_4$ or in water are not grouped together in well-defined domains, but are distributed evenly over the whole protein.

One of the most interesting hydrophobic residues is Phe87 which had the highest flexibility of all residues in the lid region. Superimposition of the averaged structure from five simulations of open CRL to the crystal structure showed that in $CCl_4$ this side chain get exposed to the solvent while it remained buried in the water simulation. Another interesting residue is the oxyanion hole residue Gly124 [7] which became highly flexible in open CRL in water.

For closed CRL, B-factors calculated from the simulations were also lower than the crystallographic values. In the water simulation, surface-exposed and hydrophilic residues were more flexible (Fig. 4a): Asn8, Gly9, Asp10, Ser47, Lys52, Lys75, Met82, Glu88, Lys109, Glu208, Lys231, Glu257, Ser272, Asn292, Leu302, Arg324, Glu360, Glu364, Asp392, Ile395, Tyr458, Leu486, Lys488, Glu491, Asn506 and Leu510, while in the simulations in $CCl_4$ B-factors were larger for surface-exposed and hydrophobic residues (Fig. 4b): Ile18, Asp191, Met244, Met319, Ile395-Leu399, Tyr458, Leu486, Leu508 to Leu510 and Phe526.

As for open CRL, closed CRL generally had similar flexibility in water and $CCl_4$. However, the number of flexible residues in water is larger than the number of flexible

residues in $CCl_4$. Direct comparison of simulations in water and $CCl_4$ of closed CRL showed that 26 mostly hydrophobic residues were more flexible in $CCl_4$, while 88 mostly polar residues were more flexible in water (Fig. 5b). Eleven residues with higher flexibility in $CCl_4$ (Leu114, Asp191, Met216, Met244, Leu297, Met319, Leu413, Leu485, Met503, Phe526 and Phe533) and 7 residues with higher flexibility in water (Asp10, Lys180, Asn265, Leu302, Asn314, Leu410 and Asp515) were buried. In 14 residues the flexibility of backbone atoms was affected: Ala1, Ala7, Asn8, Gly9, Ser45, Gly46, Ala76, Pro106, Ala110, Gly269, Ser270, Ala271, Ser272 and Val487 (Fig. 6b).

Time-correlation analysis of lid movements

During the simulation the position of the lid slowly varied. The motion of the lid (residues 75-84) was analysed as a co-operative, rigid body movement relative to the protein core (residues 1-61 and 93-534). The position of the lid is characterized by a vector from the center of mass of the protein core to the center of mass of the lid.

For open CRL in water the time correlation function of this vector showed one exponential decay with a correlation time $\tau$ = 93 ps and an amplitude C = 0.09 (Fig. 7a). In contrast, for simulations in $CCl_4$ the lid had a more complex dynamics. Exponential fit of open CRL in $CCl_4$ resulted in two $\tau$ values: a fast motion $\tau_1$ = 5.6 ps ($C_1$ = 0.0019) and a slow motion $\tau_2$ = 164 ps ($C_2$ = 0.0041) (Fig. 7b).

For closed CRL the lid showed similar amplitudes and correlation times in both solvents: in water $\tau_1$ = 6.1 ps ($C_1$ = 0.0018) and $\tau_2$ = 175 ps ($C_2$ = 0.0047) (Figure 8a), while in $CCl_4$ $\tau_1$ = 4.6 ps ($C_1$ = 0.0014) and $\tau_2$ = 132 ps ($C_2$ = 0.0059) (Fig. 8b).

From the amplitude of the exponential decay, the maximum angle of lid movement $\theta_{ij}(t\rightarrow\infty)$ can be calculated by Equation 4 and the maximum displacement d by Equation 5. In the open CRL, the maximum displacement differed considerably in $CCl_4$ and in water: 0.9 Å

and 1.6 Å, respectively. This stabilizing effect of organic solvent was not observed in closed CRL. Both simulations in water and $CCl_4$ show similar scalar displacements of 1.1 Å

The role of Lys85 and Lys75

What is the molecular mechanism which leads to the decreased mobility of the open lid in $CCl_4$? Analysis of averaged structure of open CRL in both solvents pointed to the role of Lys85. This residue is located at the center of the lid and is surface-exposed in the open crystallized structure. In the water simulation Lys85 was exposed, but when simulated in $CCl_4$, Lys85 flipped back and formed a stable salt bridge to Asp284, as concluded from the short distance of 3.3 $\pm$ 0.07 Å between NZ atom of Lys85 and CG atom of Asp284. In contrast, open CRL simulated in water was lacking this salt bridge with distance of 15.3 $\pm$ 1.3 Å between Lys85 and Asp284 (Fig. 6a and Fig. 9a).

Another lid-locking mechanism found in open CRL is a hydrogen bond between Lys75 and Asn292. [12] This hydrogen bond was maintained in five water simulations with the distance of 3.3 $\pm$ 0.3 Å between NZ atom of Lys75 and OD1 atom of Asn292 (Fig. 6a and Fig. 9c). In $CCl_4$, two of five simulations in $CCl_4$ showed a hydrogen bond between Lys75 and Asn292 with the distance of 3.0 $\pm$ 0.1 Å, while in the other three simulations a salt bridge between Lys75 and Asp79 with the distance of 3.5 $\pm$ 0.02 Å was formed (Fig. 6a and Fig. 9b). As for the Lys85-Asp284 bridge, the distances between Lys75 and Asn292 or Asp79 was generally smaller and less fluctuating in $CCl_4$ compared to the water simulation.

## Discussion

### Structure

All simulations in water had lower rmsd values compared to simulations in $CCl_4$, indicating that they deviate less from the crystal structure. These results are in agreement with Toba *et al.* [19] who found that γ-chymotrypsin was closer to its initial structure when it was simulated in water rather than in hexane. However, this observation cannot be generalized, because for BPTI they found that the deviation was larger for the water simulation. [11, 20] In the case of CRL, simulation in $CCl_4$ leads to a higher number of internal hydrogen bonds (data not shown), indicating that CRL becomes more packed. Increase of internal hydrogen bonds is also related to a decrease of the radius of gyration and solvent-accessible surface area. [21] Interestingly, lid mobility did not contribute significantly to the deviation from the initial structure. These findings support the notion that the open and closed conformations are well-defined energy minima separated by a high energy barrier, which most likely is caused by a *cis-trans* isomerization of Pro92. [8] Starting at the crystal structure, the system rapidly relaxes and then explores the accessible conformational space by a passage through a series of local minima which have a similar rmsd from the initial structure, [22] and are separated by low energy barriers. [23]

### Flexibility

It is commonly thought that water-soluble proteins are more flexible in water than in organic solvent, because water acts as “life lubricant” by hydrogen bonding networks to polar residues. [24] This higher flexibility also may be caused by reduced electrostatic interaction due to dielectric screening [25] upon solvating the polar and charged residues. [26] Lower flexibility of protein was also observed in chloroform, [11, 21] hexane, [20, 27] methyl

hexanoate, [28] dimethylformamide, acetone, butanone, tetrahydrofuran, and cyclohexane. [13] As a mechanism, Hartsough and Merz [11] proposed that in water polar and charged side chains move away from the core of the protein and thus decrease the intramolecular interactions of the protein, which are mainly hydrogen bonds and salt bridges and responsible to the rigidity of the protein.

Our findings indicate that the effect of organic solvent is not global, but solvents rather interact specifically with surface-exposed residues. In water, hydrophilic side chains become more flexible, while in organic solvent hydrophobic residues have increased flexibility. The overall effect on flexibility depends on the percentage of hydrophilic and hydrophobic residues on the protein surface. Soluble proteins like CRL in its closed form have a majority of hydrophilic residues at the protein surface, thus the overall effect of organic solvent is a decrease in flexibility. In contrast, open, activated CRL exposes a large hydrophobic patch towards the substrate interface which becomes more flexible in organic solvent. Figure 5 shows that the number of atoms above the y=x line, *i.e.* the atoms which are more flexible in $CCl_4$, is much less in closed CRL than in open CRL. This observation suggests that instead of exerting a global effect on protein flexibility, organic solvents specifically act on individual residues.

Changes of flexibility seem to be restricted to side chains, while the backbone is hardly affected. In addition, the overall structure is similar in both solvents, as it has been previously found comparing the crystal structures of subtilisin Carlsberg, *P. cepacia* lipase (PCL), and *C. antarctica* lipase B (CALB) in anhydrous solvents and in water. [9, 10, 29] For some side chains, the organic solvent mediates their orientation: Phe87, the most hydrophobic residue in the lid, points to the solvent in the $CCl_4$ simulations of open CRL, but is buried in the protein in the water simulations, similar to the crystal structure. Grochulski *et al*. [8] stated that Phe87 has numerous interactions in the closed CRL. It sticks into a hydrophobic pocket of

seven hydrophobic residues. In the open conformation it has no interaction with other residues; however, it may be interesting to consider the effect of organic solvent on the stabilization of hydrophobic part of the lid region. This mechanism of "solvating" hydrophobic side chains in hydrophobic environment was observed in *Rhizomucor miehei* lipase where the hydrophobic side chain of the residues Ile85, Ile89, and Leu92 reach and embedded in the lipid interface when the lid opens. [30]

Dynamics

In this study we focused on modelling the dynamical properties in the equilibrium states rather than of the transition between closed and open conformation, which takes place on a much longer time scale. The lid movement can be described as a diffusive motion in a potential well. This slow motion involves cooperative displacements and therefore may also be coupled to the global dynamics of the protein. [31] Analysis of time-correlation functions shows that the lid region is less flexible in $CCl_4$ as compared to water. In addition to hydrophobic stabilization of inner face of the lid, [30] this stabilization is caused by additional, specific interactions in organic solvent: two salt bridges Lys85-Asp284 and Lys75-Asp79, and a hydrogen bond Lys75-Asn292. A related lid-locking mechanism involving a tryptophan residue [32] and arginine [33] were reported for *Rhizomucor miehei* lipase. Stabilization of open conformation of the lid may also come from hydrogen bond interactions between Tyr69 and Glu70 with a glucan chain which is linked with Asn351. [34]

In summary, the present study indicates that the motions of the mobile elements of CRL are highly dependent on the solvent. A hydrophobic environment stabilizes the lid but renders the side chains in the substrate binding site more mobile. Thus, a dynamical molecular model of CRL in different solvents can help to design engineered catalysts with improved properties in organic solvents.

**Acknowledgements**

This work was supported by the German Federal Ministry of Education and Research (project WTZ-MYS 02/001) and Malaysian Ministry of Science, Technology and Environment (project IRPA 09-02-04-001/BTK/TD/004).

**References**


1. Klibanov AM (2000) Trends Biotechnol 18:85-86
2. Klibanov AM (2001) Nature 409:241-246
3. Berglund P (2001) Biomol Eng 18:13-22
4. Derewenda U, Brzozowski AM, Lawson DM, Derewenda ZS (1992) Biochemistry 31:1532-1541
5. Verger R (1997) TIBTECH 15:32-38
6. Pandey A, Benjamin S, Soccol CR, Nigam P, Krieger N, Soccol VT (1999) Biotechnol Appl Biochem 29:119-131
7. Grochulski P, Li Y, Schrag JD, Bouthillier F, Smith P, Harrison D, Rubin B, Cygler M (1993) J Biol Chem 268(17):12843-12847
8. Grochulski P, Li Y, Schrag JD, Cygler M (1994) Prot Sci 3:82-91
9. Secundo F, Carrea G (2002) J Mol Catal B 19-20:93-102
10. Schmitke JL, Stern LJ, Klibanov AM (1997) Proc Natl Acad Sci USA 94:4250-4255
11. Hartsough DS, Merz KM (1992) J Am Chem Soc 114:10113-10116
12. Weber HK, Zuegg J, Faber K, Pleiss J (1997) J Mol Catal B 3:131-138
13. Broos J, Visser AJWG, Engbersen JFJ, Verboom W, van Hoek A, Reinhoudt DN (1995) J Am Chem Soc 117(51):12657-12663
14. Case DA, Pearlman DA, Caldwell JW, Cheatham III TE, Wang J, Ross WS, Simmerling CL, Darden TA, Merz KM, Stanton RV, Cheng AL, Vincent JJ, Crowley M, Tsui V, Gohlke H, Radmer RJ, Duan Y, Pitera J, Massova I, Seibel GL, Singh UC, Weiner PK, Kollman PA (2002) AMBER 7, University of California, San Francisco
15. Berman HM, Westbrook J, Feng Z, Gilliland G, Bhat TN, Weissig H, Shindyalov IN, Bourne P E (2000) Nucleic Acids Res 28:235-242
16. Fox T, Kollman PA (1998) J Phys Chem B 102:8070-8079

17. Ryckaert JP, Ciccotti G, Berendsen HJC (1977) J Comput Phys 23:327-341
18. Darden T, York D, Pedersen L (1993) J Chem Phys 98:10089-10092
19. Toba S, Hartsough DS, Merz KM (1996) J Am Chem Soc 118:6490-6498
20. Hartsough DS, Merz KM (1993) J Am Chem Soc 115:6529-6537
21. Peters GH, van Aalten DM, Edholm O, Toxvaerd S, Bywater R (1996) Biophys J 71(5):2245-2255
22. Mikhailov D, Linhardt RJ, Mayo KH (1997) Biochem J 328:51–61
23. Sinha N, Kumar S, Nussinov R (2001) Structure 9:1165-1181
24. Barron LD, Hecht L, Wilson G (1997) Biochemistry 36(43):13143-13147
25. Brooks III CL Karplus M (1989) J Mol Biol 208(1):159-181
26. Bone S (1987) Biochim Biophys Acta 916:128-134
27. Soares CM, Teixeira VH Baptista AM (2003) Biophys J 84:1628-1641
28. Norin M, Haeffner F, Hult K, Edholm O (1994) Biophys J 67(2):548-559
29. Mattos S, Ringe D (2001) Curr Opin Struct Biol 11:761-764
30. Peters GH, Bywater RP (2001) Biophys J 81:3052-3065
31. Shen M, Freed KF (2002) Biophys J 82:1791-1808
32. Norin M, Ohlsen O, Svendsen A, Edholm O, Hult K. (1993) Protein Eng 6:855-863
33. Holmquist M, Norin M, Hult K (1993) Lipids 28(8):721-726
34. Brocca S, Persson M, Wehtje E, Adlercreutz P, Alberghina L, Lotti M (2000) Protein Sci 9:985-990

**Figure captions**

**Fig. 1.** Superimposition of open (black, PDB entry 1CRL) and closed (grey, PDB entry 1TRH) conformers of *C. rugosa* lipase. The mobile lid is indicated.

**Fig. 2. a)** rmsd of a 1000 ps CRL simulation (closed form, solvent $CCl_4$) from the X-ray structure; **b)** two-dimensional rmsd plot of the same simulation; conformers with a deviation of less than 0.7 Å (green) are considered as conformers in a local minimum

**Fig. 3.** Comparison of simulated (black) and crystallographic (red, PDB entry 1CRL) B-factors of open CRL simulated in water **(a)** and $CCl_4$ **(b)**. The lid is indicated by a blue line.

**Fig. 4.** Comparison of simulated (black) and crystallographic (red, PDB entry 1TRH) B-factors of closed CRL simulated in water **(a)** and $CCl_4$ **(b)**. The lid is indicated by a blue line.

**Fig. 5.** Correlation plot of simulated B-factors for open **(a)** and closed **(b)** CRL simulated in water and $CCl_4$. High B-factors of water simulations which correlate with low B-factors of $CCl_4$ simulations are inside the blue box and high B-factors of $CCl_4$ simulations which correlate with low B-factors of water simulations are inside the red box.

**Fig. 6**. Stereo view of open **(a)** and closed **(b**) conformation of CRL. Residues which are more flexible in water (blue) or more flexible in $CCl_4$ (red) are derived from Figure 5. Residues which are mentioned in the text are labelled. The three bridges which lead to the lid locking mechanism (Lys85-Asp284, Lys75-Asp79, and Lys75-Asn292) are displayed and marked blue (structure in water) and red (structure in $CCl_4$) (inset).

**Fig. 7.** Time-correlation functions of open CRL simulated in water **(a)** and in $CCl_4$ **(b)**. The fitted exponential is indicated (----).

**Fig. 8.** Time-correlation functions of closed CRL simulated in water **(a)** and in $CCl_4$ **(b**). The fitted exponential is indicated (----).

**Fig. 9.** Time dependence of the distance Lys85-Asp284 **(a)**, Lys75-Asp79 **(b)**, and Lys75-Asn292 **(c)** in water (red) and in $CCl_4$ (black).

**Figure 1:**

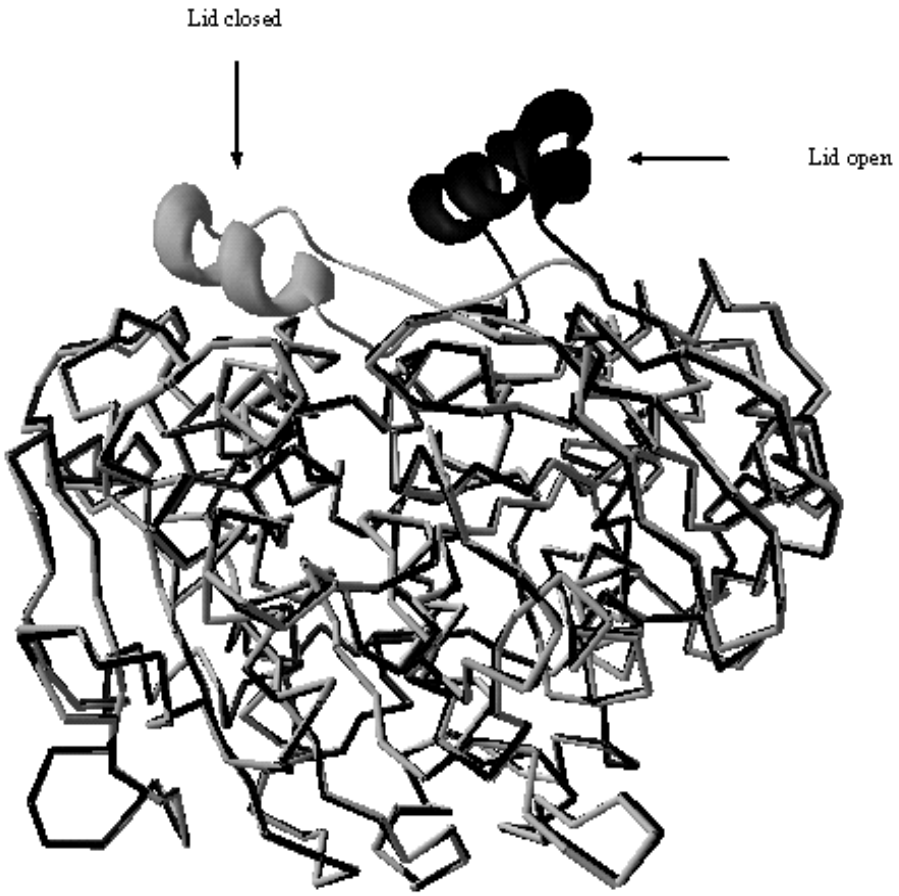


**Figure 2A:**

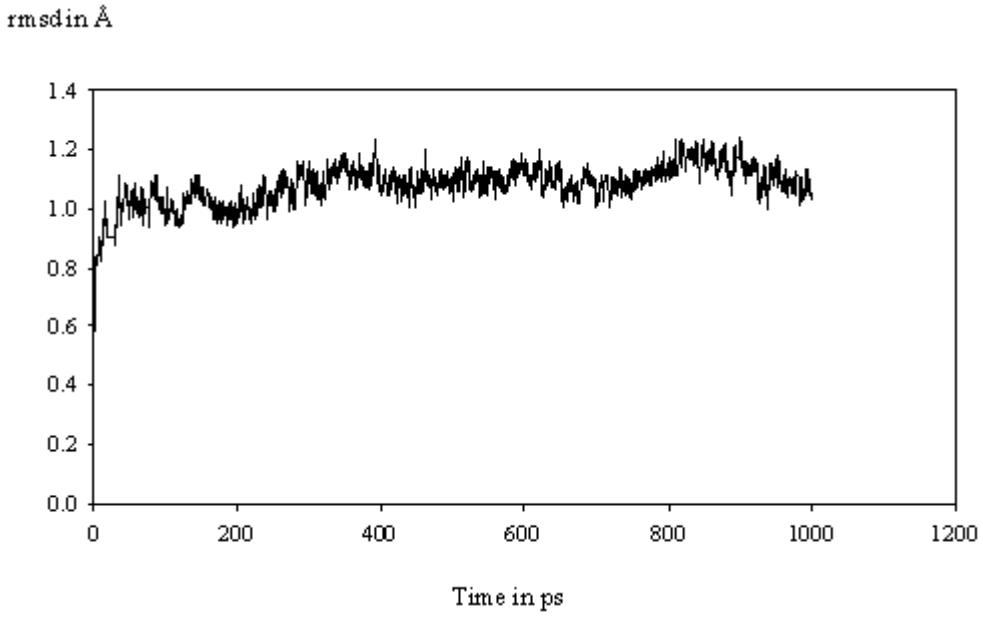

**Figure 2B:**

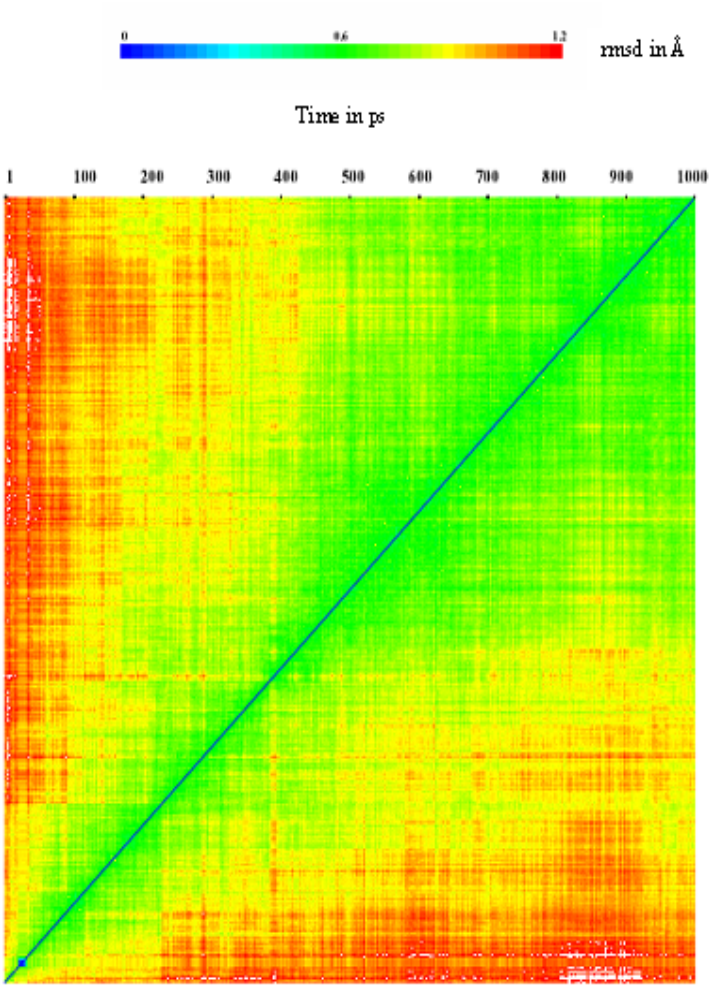


**Figure 3A:**

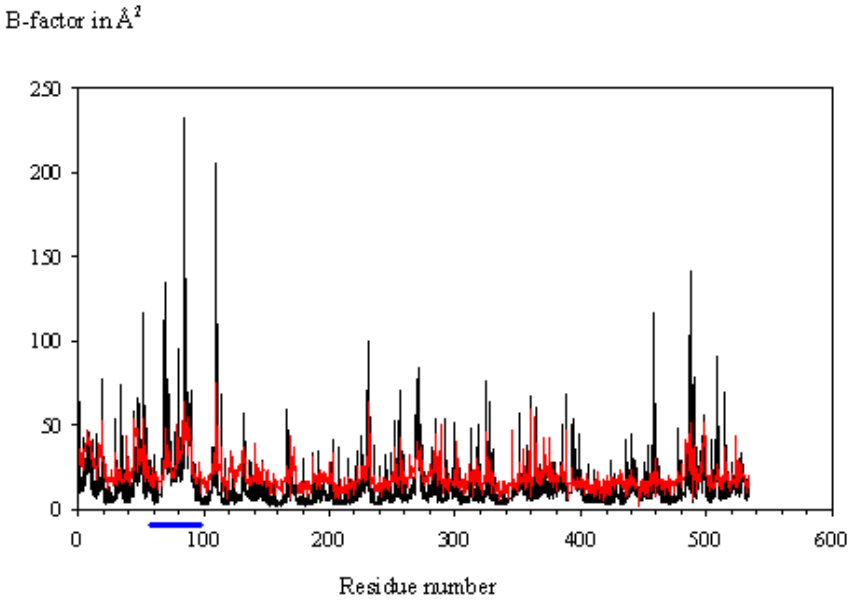

**Figure 3B:**

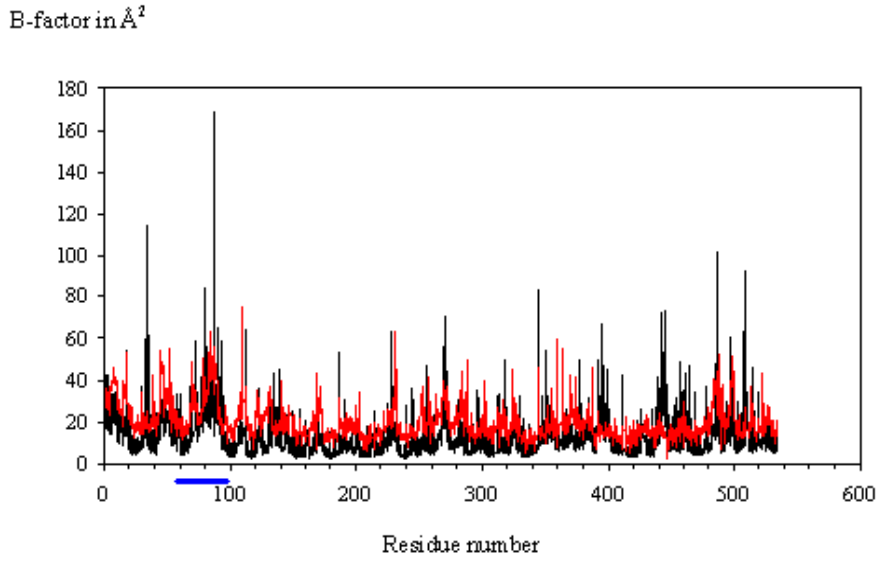


**Figure 4A:**

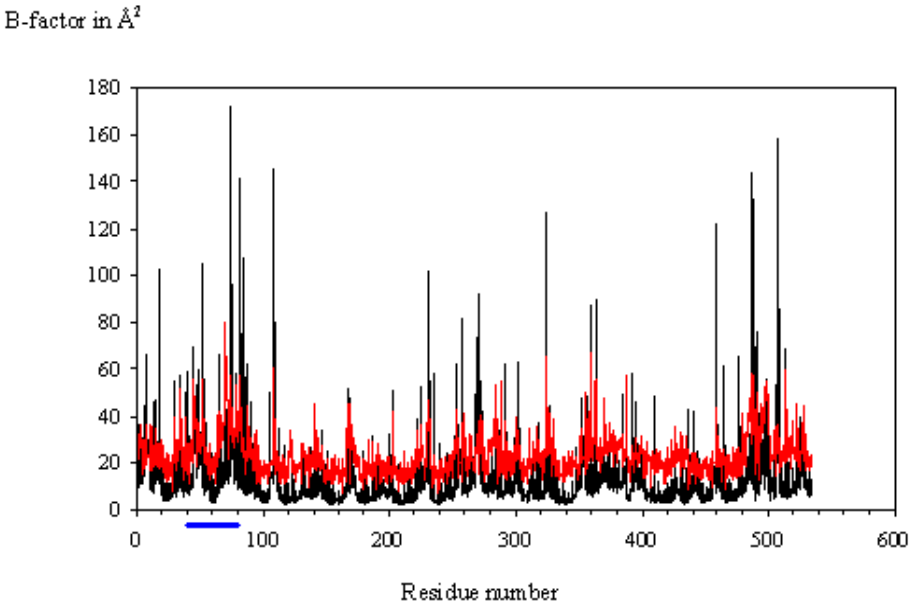

**Figure 4B:**

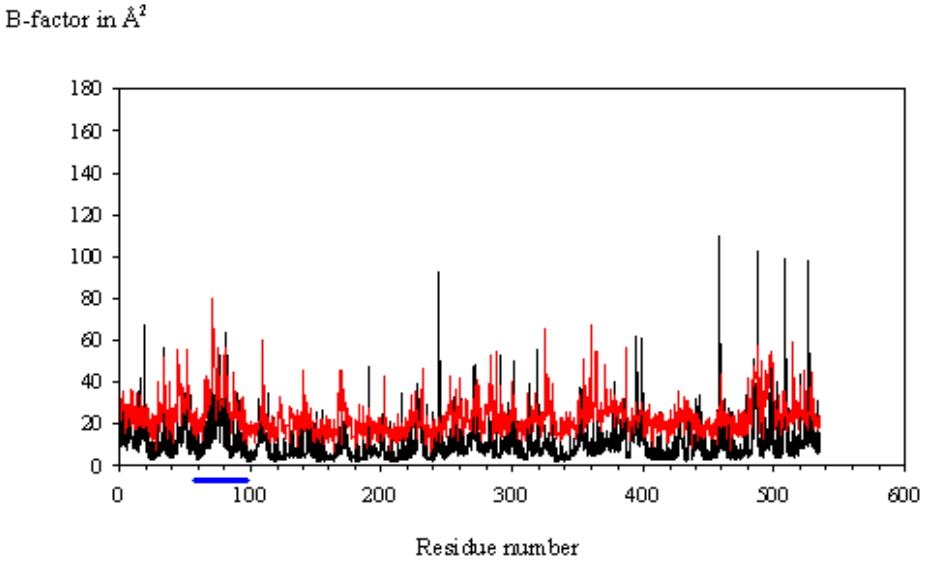


**Figure 5A:**

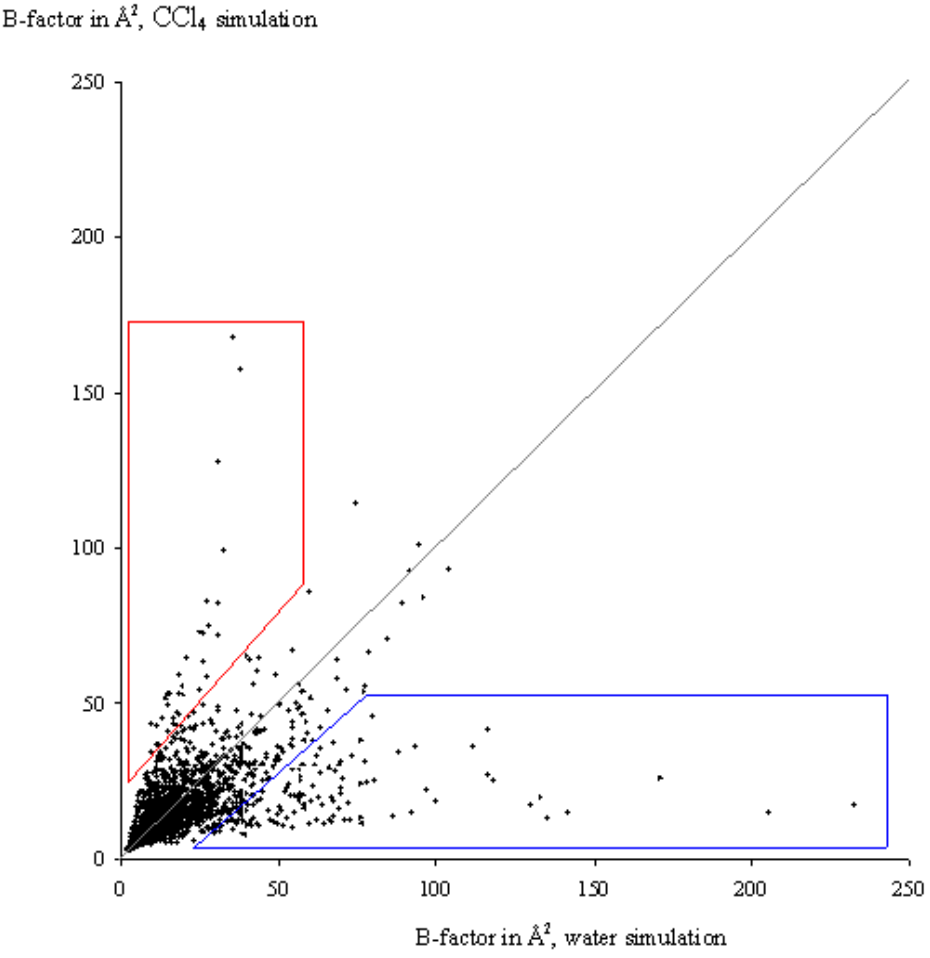

**Figure 5B:**

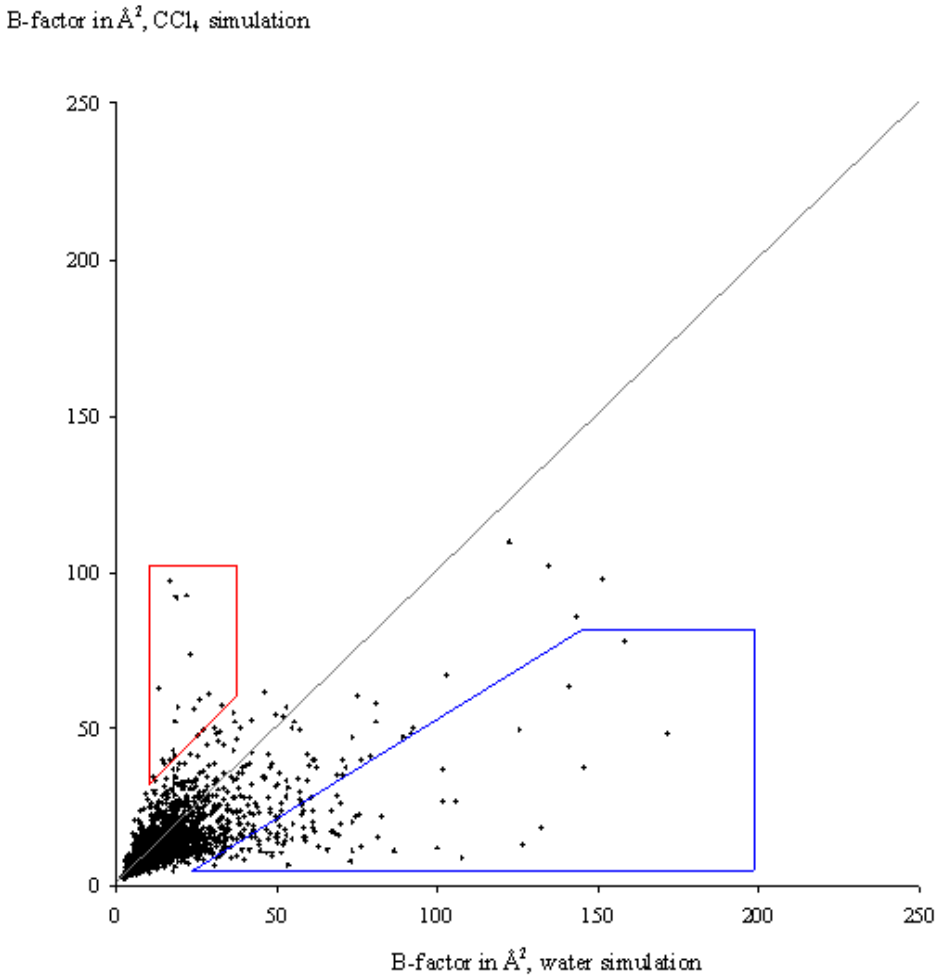
B-factor in Å², CCl4 simulation
250
200
150
100
50
0
0
50
100
150
200
250
B-factor in Å², water simulation

**Figure 6A:**

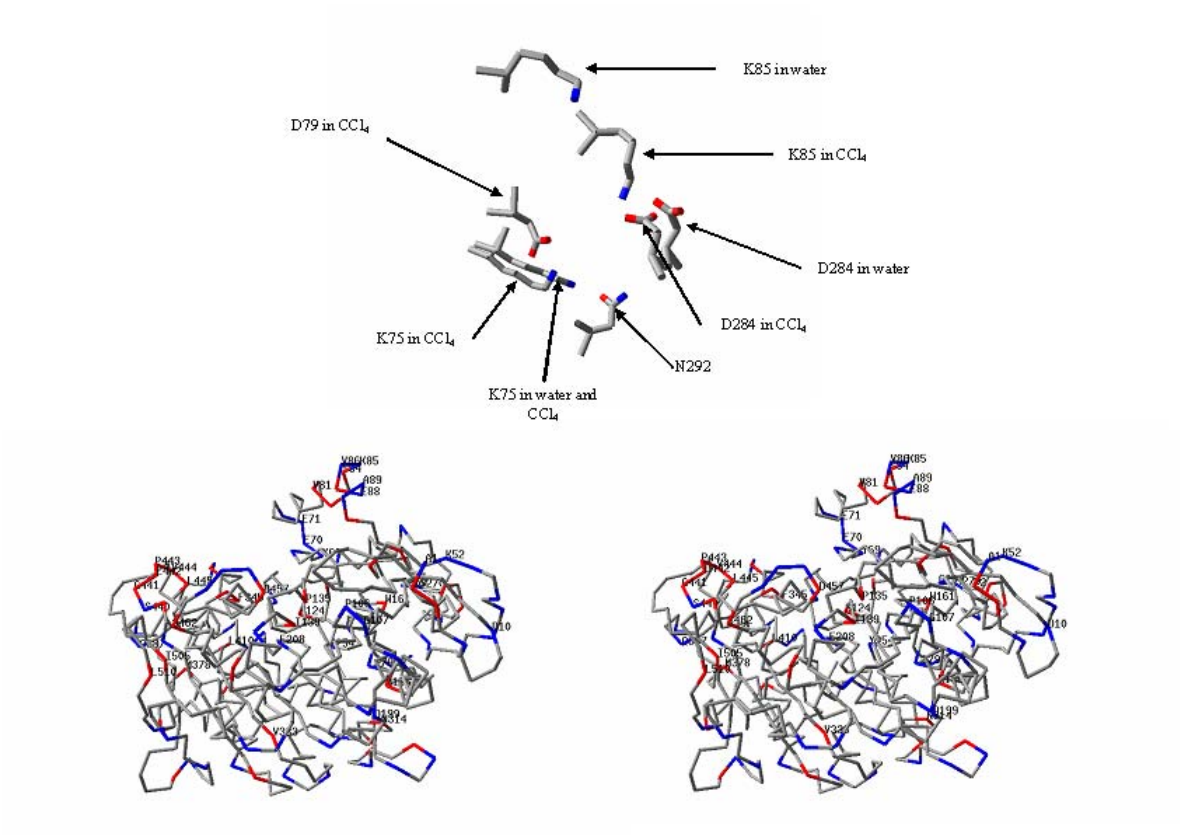


**Figure 6B:**

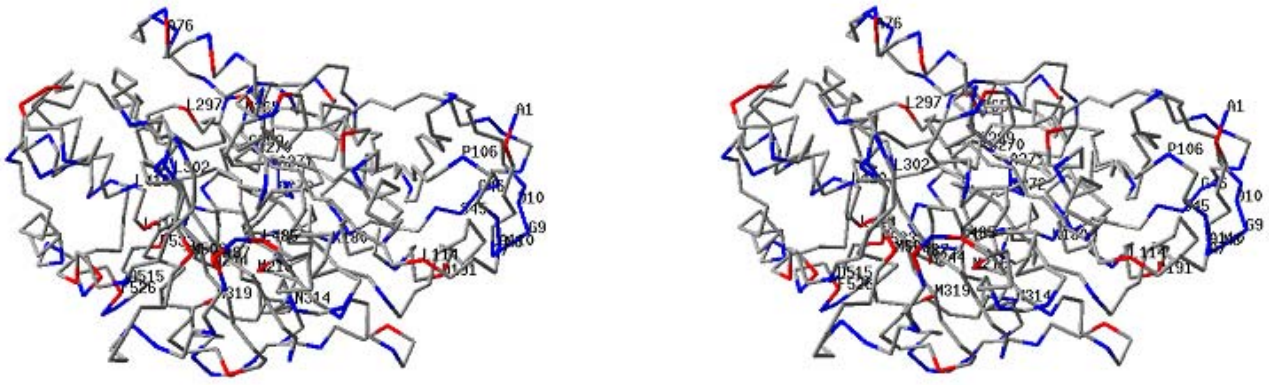

**Figure 7A:**

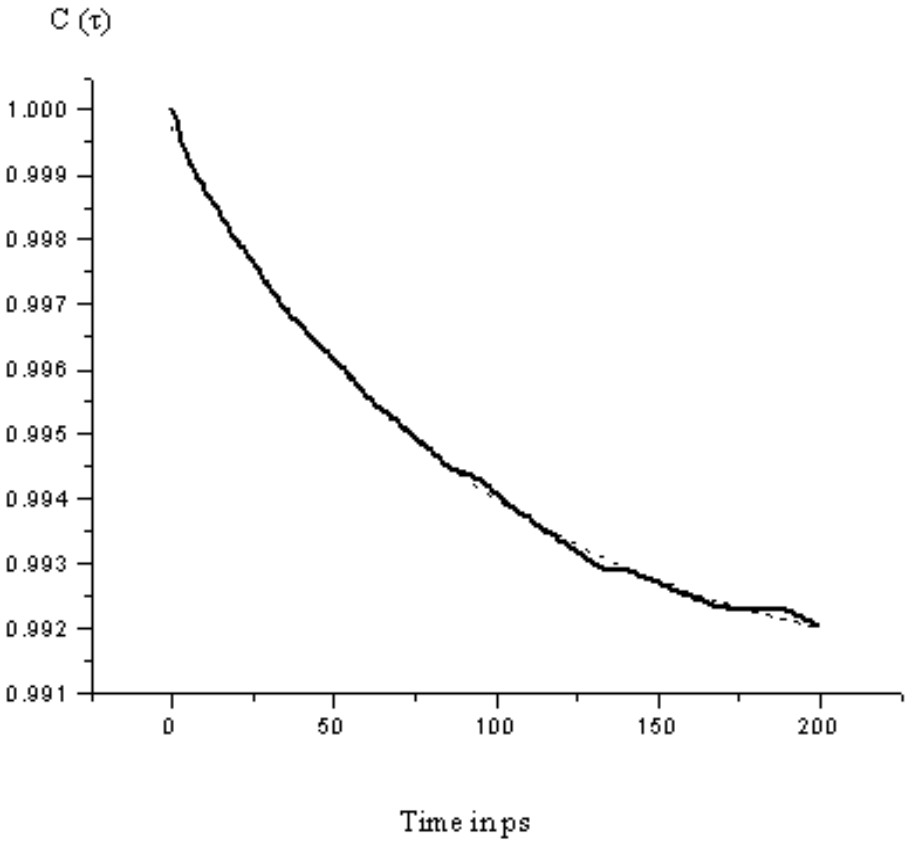


**Figure 7B:**

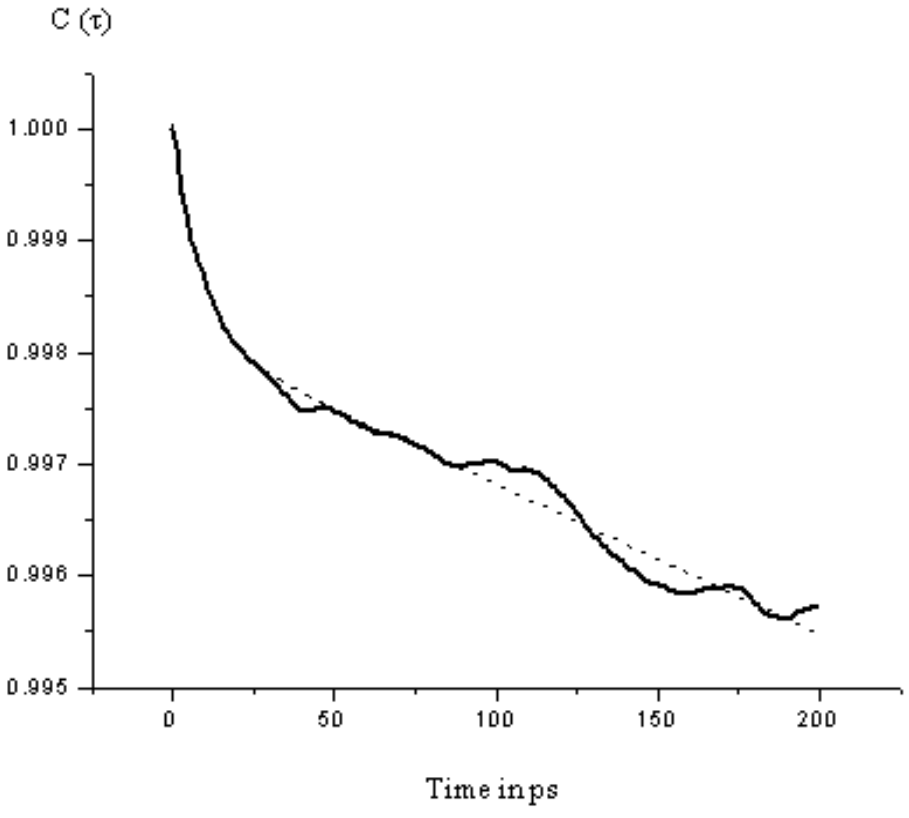

**Figure 8A:**

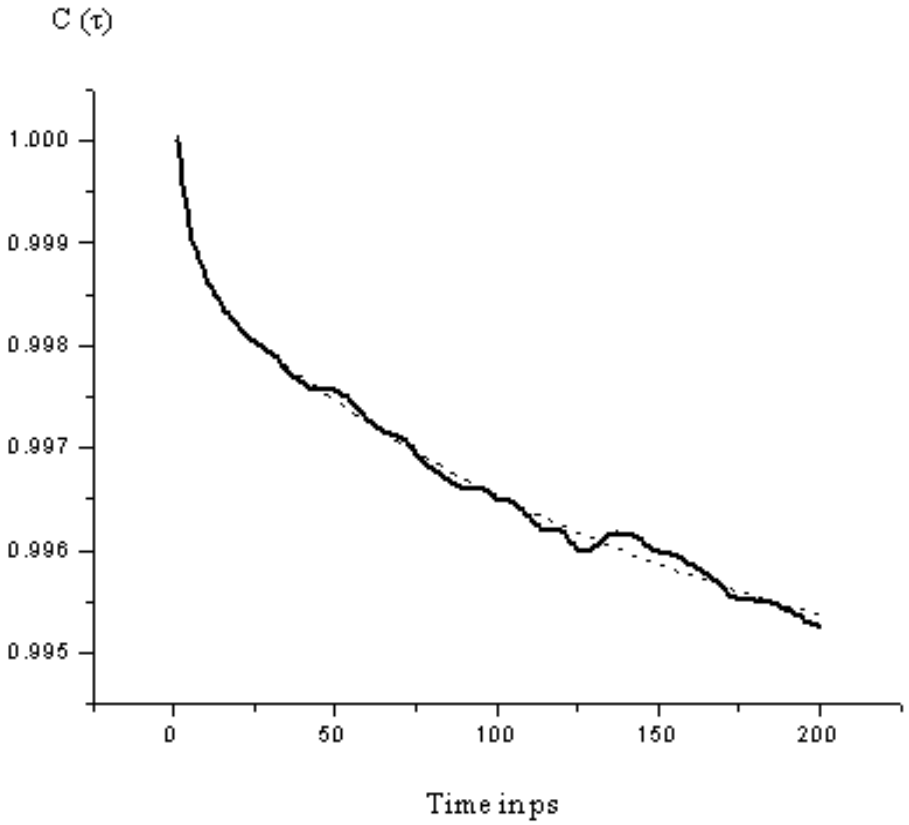


**Figure 8B:**

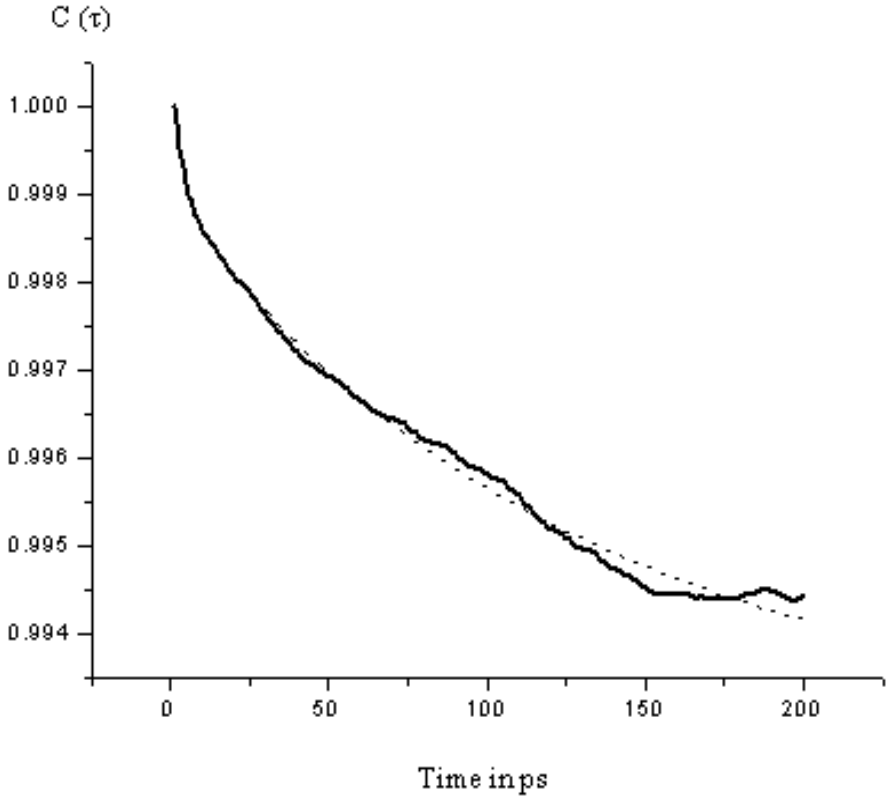

**Figure 9A:**

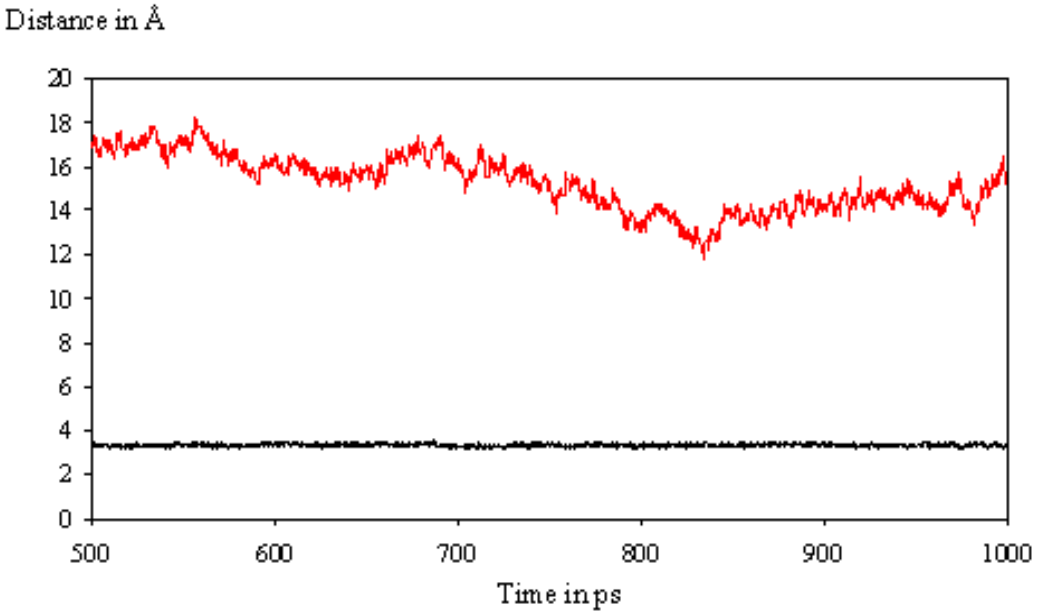


**Figure 9B:**

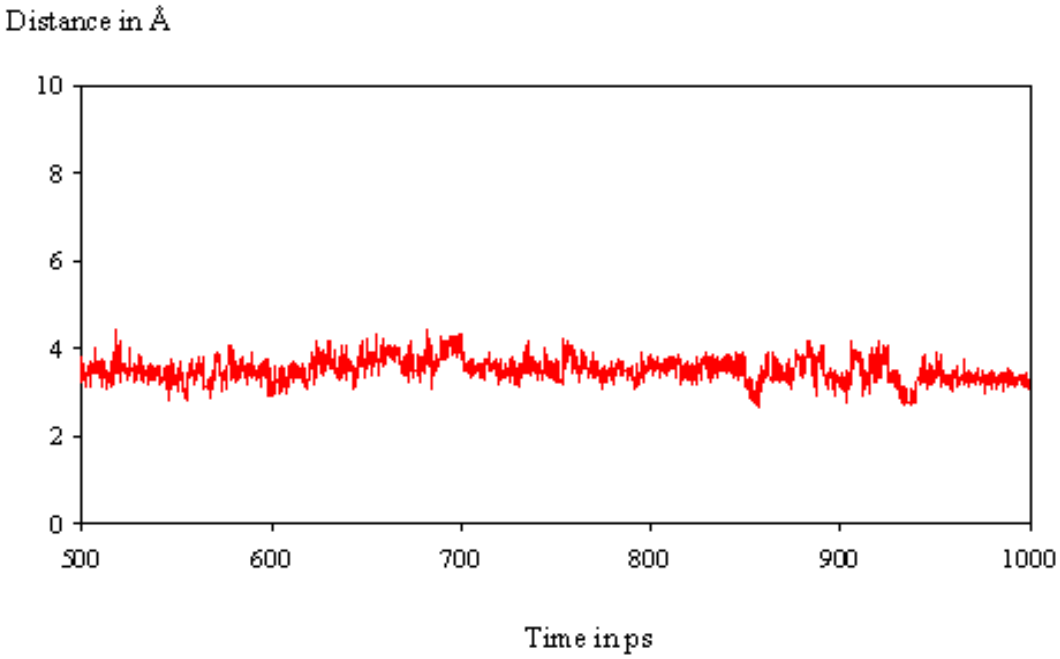

**Figure 9C:**